Local Dynamics and Glass Transition

Burak Erman
Sabanci University, Sabanci Center, 80745 Istanbul Turkey

Ivet Bahar
Polymer Research Center and Chemical Engineering Department, Bogazici University, and TUBITAK Advanced Polymeric Materials Research Center, Bebek 80815, Istanbul, Turkey

SUMMARY: The dynamics of polymer chains in the bulk state are discussed at three different temperature scales: (i) Well above the glass transition temperature where the basic step of motion is the rotameric transition of bonds. In this regime, the dynamics may conveniently be analyzed by the rotational isomeric state model. (ii) In the vicinity of glass transition where friction forces from the environment dominate. In this regime, the dynamics may be modeled according to the cooperative kinematics model. (iii) Well below glass transition. Here, an analogy with a native protein is made, and the mean-squared fluctuations are analyzed by adopting the Gaussian Network Model, which recently proved successful in describing fluctuations in native proteins.

Introduction

The dynamics of polymer chains in the bulk state may be studied in three different temperature ranges: (i) well above the glass transition temperature, T_g, (ii) in the immediate vicinity of T_g, and (iii) well below T_g. This artificial but helpful classification allows us to focus on different aspects of chain dynamics without introducing a general but complicated model.

The dynamics of polymer chains on a local scale in the bulk state above glass transition is now well understood. The basic step of motion is the rotameric transition of bonds. The internal barriers to backbone rotameric jumps play a dominant role in controlling the kinetics of conformational motions in this regime, as suitably described by dynamic rotational isomeric state model and calculations.[1,2] The isomeric jumps may result in substantial changes in bond positions and orientations.

 CCC 1022-1360/98/$ 17.50

In general, bond rotational jumps are intramolecularly coupled to librational motions about rotameric minima, as well as to fluctuations in bond lengths and bond angles. Intermolecularly, they are coupled to their immediate environment. The environment imposes a resistance to rotameric transitions since each transition has to be accompanied by the displacements of pendant groups of atoms. Although such intermolecular constraints are relatively weak well above T_g, it is now widely established that their influence increases as T_g is approached; and these eventually dominate the rate and mechanism of motion in the vicinity of T_g. A strong cooperativity between the various internal degrees of freedom of the chain emerges in this second temperature range, which ensures the most efficient *localization* of the motion driven by an isomeric jump. Results of computer simulations [3-6], as well as cooperative kinematics [7-11] calculations exhibit a close agreement, consistent with experimental observations,[12] on the correlation length and localization mechanism of motions in highly restrictive environment, : A rotameric transition can take place only if a few bonds on both sides of the rotating bond along the chain readjust in space.

At the other end of the spectrum, the dynamics of polymers in the bulk state well below T_g is essentially dominated by thermal fluctuations, described by the Debye-Waller factors [13]. Fluctuations of the backbone atoms are strongly correlated with the local density. However, cooperativity of much larger length scales can also be identified for these systems, as will be discussed in detail below.

Dynamics well above Tg

A crossover from independent to cooperative segmental dynamics in poly(vinyl chloride) has been observed in quasielastic neutron scattering experiments by Colmenero et. al.[14] This crossover takes place at a time t_C below which a single exponential relaxation occurs, and above which the dynamics of the system becomes cooperative and obeys a stretched exponential behavior. The relaxation function $\phi(t)$ associated with a time-dependent local variable may thus be written as

$$\phi(t) = \begin{cases} \exp(-t/\tau_D) & t < t_C \\ \varphi(t) & t > t_C \end{cases} \qquad (1)$$

where τ_D is the relaxation time for the single exponential behavior, and $\varphi(t)$ is the decay function conveniently represented by the Kohlrausch-Williams-Watts (KWW) expression $\exp[-(t/\tau)^{\beta}]$, with the exponent β less than unity. One may define in an operative way a temperature T^* at which $\tau_D = t_C$. Inelastic neutron scattering experiments on PVC [14] lead to a value of $T^* = 760°K$.

Accepting the existence of a discrete crossover time separating the Debye and non-Debye types of relaxation, one is now confronted with the question of elucidating the molecular aspects of the motion in the two regimes. One possible interpretation is to introduce a correlation time τ_c associated with local motions during an isomerization transition as [2, 7]

$$\tau_c \sim [\, \xi \sum_i \delta R_i \bullet \delta R_i \,] \exp \{\Delta V/RT\} \qquad (2)$$

Here, ξ is the friction coefficient, $\sum_i \delta R_i \bullet \delta R_i$ is the total squared displacement of atoms accompanying the rotameric transition, and ΔV is the "effective" potential energy barrier to be surmounted during the transition. The term effective is used here, because, in addition to the conformational change of the isomerizing bond, ΔV contains contributions from induced changes in the torsional states of all neighboring bonds as well as excluded volume type interactions among near (sequentially) neighboring atoms of the chain. The correlation time given in eq 2 may suitably be associated with the reorientations of bonds observed in NMR experiments[15]. Above the crossover temperature T^*, the exponential term in eq 2 will dominate.[16], while at lower temperature, or longer time scales, the mechanism of motion should be properly adjusted to minimize the atomic displacements, and the type of motion which achieves the most efficient localization of conformational change is selected.

An alternative molecular rationale for the occurrence of a single exponential decay at short times, followed by a stretched exponential relaxation at longer times, is based on the dynamic rotational isomeric state approach [1, 2]. The latter uses a master equation formalism for describing the stochastics of transitions between isomeric states, such that

$$\partial \mathbf{P}(\Omega) / \partial t = \mathbf{A}\, \mathbf{P}(\Omega) \qquad (3)$$

Here $\mathbf{P}(\Omega)$ is the v^m dimensional vector of the probabilities of occurrence of the v^m isomeric conformations accessible to a segment of m bonds, each bond assuming v possible isomeric states, and **A** is the transition matrix of the rate constants governing the passage between those isomeric conformations. The ijth off-diagonal element of **A** represents the rate constant associated with the transition from conformation j to conformation i, usually given by Kramers' rate expression; and the ith diagonal element, found from the negative sum of all elements in the corresponding column, accounts for the rate of escape from conformation i, in conformity with the detailed balance principle. The formal solution to eq (3) reads

$$\mathbf{P}(\Omega) = \exp\{\mathbf{A}t\}\ \mathbf{P}_o(\Omega) = \mathbf{B} \exp\{\Lambda t\}\ \mathbf{B}^{-1}\ \mathbf{P}_o(\Omega) \qquad (4)$$

where $\mathbf{P}_o(\Omega)$ is the vector of equilibrium probabilities, Λ is the diagonal matrix of the eigenvalues of **A**, and **B** is the matrix of the eigenvectors. Using the elements λ_i and B_{ij} of Λ and **B**, the time evolution of $\phi(t)$ may be expressed as

$$\phi(t) = \sum_i k_i \exp\{-\lambda_i t\} \qquad (5)$$

where the amplitude factor k_i is given by[2)]

$$k_i = \sum_m \sum_n B_{mi}\ [B^{-1}]_{in}\ P_o(\Omega_n)\ \phi(\Omega_m; \Omega_n) \qquad (6)$$

Here $\phi(\Omega_m; \Omega_n)$ represents the value assumed by the investigated variable, as the chain undergoes a conformational change from Ω_n to Ω_m. When plotted against time, eq 6 yields a KWW type of curve. At short times, the largest eigenvalue corresponding to the fastest mode will be the dominant contributor to relaxation and $\phi(t)$ will be a single exponential function.

Results of calculations for the dielectric response function for *cis*-polyisoprene in the bulk state, based on the above arguments are shown in Figure 1 [17)]. The ordinate and abscissa represent the KWW coordinates.

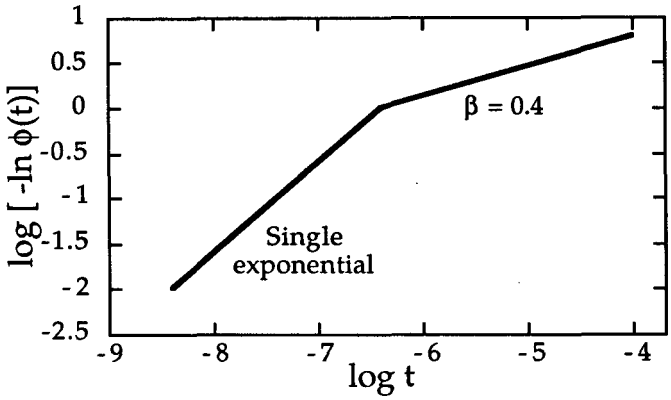

Figure 1: KWW plot of relaxation function $\phi(t)$.

Calculations are performed for the relaxation of a dipole moment vector at the end of two repeat units of polyisoprene, i.e. $\phi(t)$ represents the correlation function associated with the dipole reorientation. The separation of the curve into a single exponential and a KWW branch with $\beta = 0.4$ is observed. The exponent β was found to decrease with increasing size of the segment subject to cooperative relaxation. In fact, the exponent decreases from 0.62 to 0.35 as the size of the moving segment increases from one repeat unit (four bonds) to three (12 backbone bonds) [18].

Cooperative local dynamics

As the constraints imposed by intermolecular effects increase, cooperative motions are expected to take place so as to minimize the work done against friction while passing over saddle points of the potential energy surface. The work done against friction during differential displacements δR_i of chain atoms may be approximated as

$$\delta W \equiv (\xi / \delta t) \sum_i \delta R_i \,.\, \delta R_i \qquad (7)$$

where δt is the time step involved in this change. As a result of chain connectivity

and energy (internal conformational energy and work) requirements, local motions take place in a highly cooperative manner. The dynamics in this case is satisfactorily analyzed by the *cooperative kinematics* method[7, 10, 11, 19, 20].
The analysis of motions for a polyethylene (PE) chain in a restrictive environment shows that the immediate environment of the rotating bond undergoes coupled changes in dihedral angles so as to accommodate the new orientation imparted by the isomeric jump. In Figure 2, the coupled fluctuations in dihedral angles, following a 120° rotation in the middle bond are presented. Calculations are performed for a 24 bond PE chain [19]. The rotation was imposed on the 13th bond. Changes in the dihedral angle of the other bonds are shown along the ordinate. Cooperative changes to accommodate the rotation of the 13th bond are confined to the bonds from 9-16 . In Figure 3, the absolute displacements of bonds following the isomerization of the 13th bond are shown [19]. Again, most of the displacements to accommodate the isomerization are confined to a segment

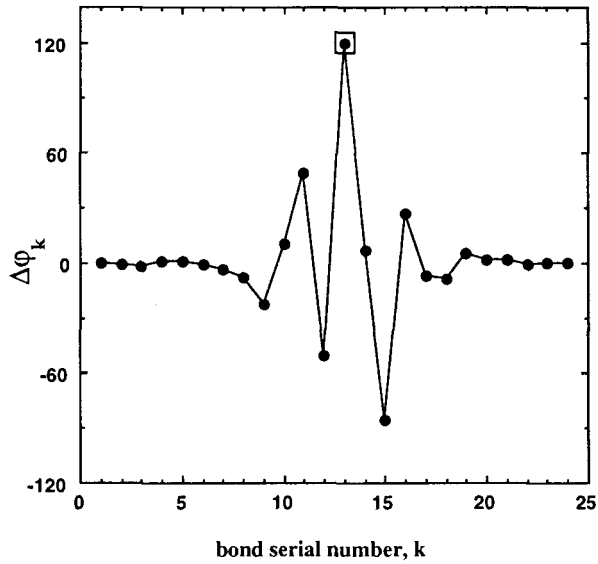

Figure 2. Torsional displacements of bonds in a 25 bond chain, resulting from a 120° isomerization of the middle bond.

of about eight bonds flanking the rotating bond. We note that the displacements of the remaining bonds outside this region do not decay to zero, and a small but finite displacement remains. The reader is referred to our previous studies, in which the results of cooperative kinematics calculations are shown[10, 11, 20] to be in excellent agreement with results from molecular dynamics (MD) simulations [4, 5, 21]. MD analysis of local dynamics of polyisoprene in the bulk state by Moe and Ediger[21] showed that cooperativity is confined to one or two repeat units. Experiments show that the same order of cooperativity is involved in glass transition[22].

Dynamics well below Tg: Native proteins carry significant information

Large scale torsional motions of dihedral angles and the resulting large scale displacements of atoms are suppressed at temperatures well below T_g. Only thermal fluctuations are present. The mean-square deviations (msd) $<\Delta R^2>$ of

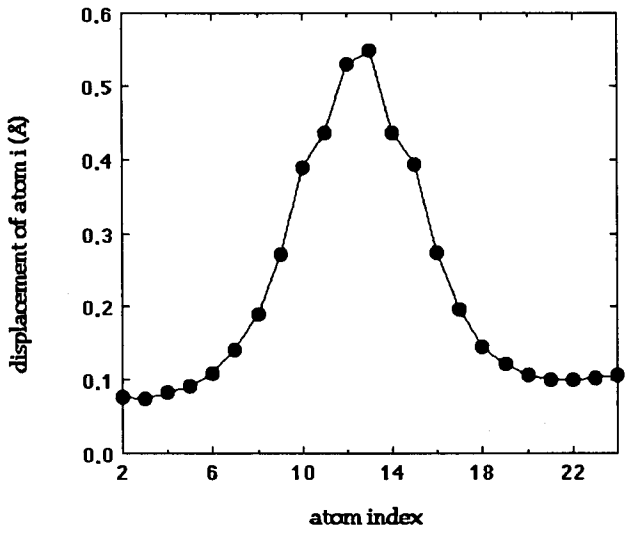

Figure 3: Displacement of backbone atoms, following the torsion of the middle bond.

atoms from their mean positions, also referred to as Debye-Waller factors or crystallographic temperature factors [13], are measured by X-ray crystallography. The Brookhaven Protein Data Bank (PDB)[23] lists the Debye-Waller factors of the atoms for more than 4000 proteins.

In Figure 4, msd values for the C^{α} atoms of the protein HIV-1 protease are plotted as a function of residue index [24]. This protein consists of two identical molecules (monomers), each of 99 residues. C^{α} atoms are the backbone carbon atoms to which amino acid side chains are attached. The residue index shown on the abscissa indicates the location of the C^{α} atom along the sequence, starting from the N-terminus. The dashed curve shows the X-ray crystallographic data reported in PDB.

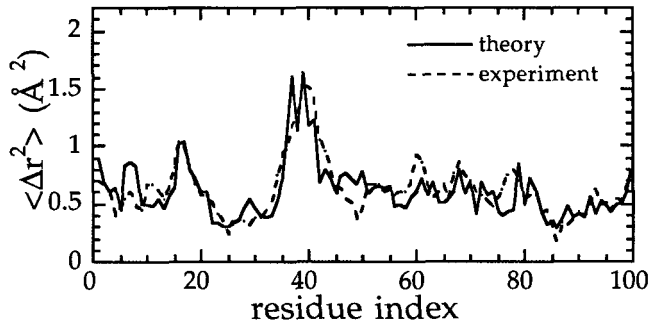

Figure 4. Fluctuations of the backbone carbon atoms of HIV-1 protease.

A protein molecule in its native state is a small system, commonly accepted to be trapped in a potential energy minimum of its phase space. Researchers refer to a protein molecule as a single glassy system and make the protein-glass analogy [25-27]. Here, we do not participate in the functional aspects of such analogies, but concentrate on the very simple common features: (i) Glasses are trapped in a region, perhaps a local minimum, of phase space [28]. The local minimum of a native protein is most probably very close to an absolute minimum. (ii) The Debye-Waller factors of glassy solids and native proteins are of the same order of magnitude [25, 29]. (iii) The local density and its fluctuations are similar in glassy

solids and native proteins. In Figure 5 the local density of the HIV-1 protease are plotted as a function of position in the molecule. The density within a spherical region of 7 Å radius is calculated at a random location in the protein. Then the point is displaced along a random direction by 0.5 Å, and the density is recalculated. Results, shown in Figure 5 are of the same order of magnitude as those of glassy solids [30].

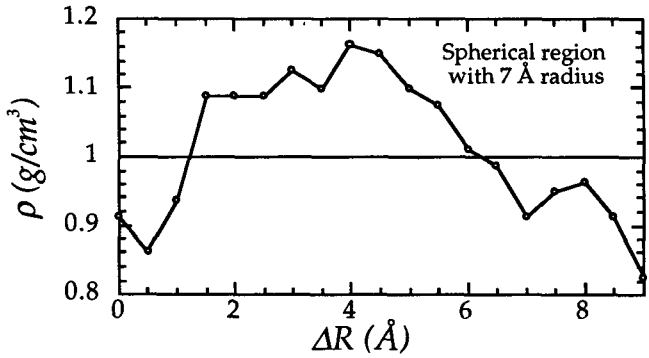

Figure 5. Local density of HIV-1 protease as a function of position.

Recently, a single-parameter Hookean potential was proposed by Tirion for the pairwise interaction of all atoms in native proteins[31]. This approximation is based on a Gaussian distribution of interatomic distances about their equilibrium values. The crystallographic temperature factors obtained by this method for G-actin bound with ADP and Ca^{++} were shown to be in close agreement with those obtained with a detailed potential introduced by Levitt[32].

The validity of a harmonic potential between residues A and B in a folded protein molecule lies in the fact that the convolution of two distribution functions may be approximated by a Gaussian. This concept is described in Figure 6. The thick curve represents the protein backbone. If residues A and B were isolated, the fluctuations in their inter-residue separation ΔR would be described by a probability distribution function $R(\Delta R)$, which is probably anharmonic, with a strong repulsion at close distances. On the other hand, both residues are under

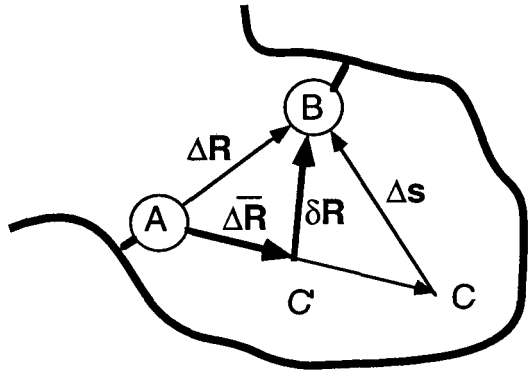

Figure 6. The interaction between residue A and B in the presence of other residues.

the joint action of all other protein residues in their neighborhood. The joint center of the potential between B and the residues in its neighborhood, other than A, is represented by the point C in the figure. Under the joint action of residue A, and all other residues, the mean position of residue B shifts to the location B' separated by a vector $\Delta\overline{\mathbf{R}}$ from A, and its fluctuation amplitudes become $\delta\mathbf{R}$. $\Delta\mathbf{s}$ is the vector denoting the instantaneous fluctuation of residue B from the center C, in the absence of A. We denote the probability distribution of $\Delta\mathbf{s}$ by $S(\Delta\mathbf{s})$. The probability distribution $P(\delta\mathbf{R})$ for the fluctuations of residue B under the joint effect of residue A and the others becomes

$$P(\delta\mathbf{R}) = R(\Delta\mathbf{R}) \times S(\Delta\mathbf{s}) \Big/ \int R(\Delta\mathbf{R}) \times S(\Delta\mathbf{s})\, d\Delta\mathbf{R} \qquad (8)$$

However, the residue A is not stationary, itself, and will be fluctuating with respect to all the other residues, i.e., with respect to point B' following the distribution $\Theta(\Delta\overline{\mathbf{R}})$. The final probability distribution of fluctuations $\Delta\mathbf{R}$ will then be given as the convolution [33]

$$R_*(\Delta\mathbf{R}) = P(\delta\mathbf{R}) * \Theta(\Delta\overline{\mathbf{R}}) \qquad (9)$$

where the symbol $*$ represents the convolution. The function R_* denotes the

probability of the inter-residue separation ΔR between residues A and B under the joint action of all residues in the neighborhood. As a result of the convolution operation, this distribution may be approximated by a Gaussian, and forms the basis of the assumption of Tirion.

Inasmuch as the time averaged positions of residues are uniquely defined in the native protein, one may make the analogy between a native protein and a Gaussian elastomeric network. The residues of the former correspond to the junctions of the latter which fluctuate about their mean positions, and the constraints imposed by Gaussianly distributed network chains correspond to the linear spring-like potentials between spatially neighboring (≤ 7.0 Å) residues. With this picture in mind, we have recently developed a Gaussian network model (GNM) of native proteins [34]. The fluctuations ΔR_{ij} in the separation $R_{ij} = | \mathbf{R}_j - \mathbf{R}_i |$ between the ith and jth C^α atoms are assumed to obey a Gaussian distribution with parameter γ^*

$$W(\Delta R_{ij}) = (\gamma^* / \pi)^{3/2} \exp(-\gamma^* \Delta R_{ij}^2) \tag{10}$$

which is equivalent to the presence of a harmonic potential $k_B T \gamma^* \Delta R_{ij}^2$ with a force constant of $2k_B T\gamma^*$. The configurational integral for a protein of N residues may be expressed, with analogy to that of random Gaussian networks[33, 35, 36] as

$$Z_N = K \exp(- \{\Delta R^T\} \Gamma \{\Delta R\}) \tag{11}$$

Here $\{\Delta R\}$ is the 3N dimensional column vector formed by the fluctuations $\{\Delta R_1, \Delta R_2, ..., \Delta R_m\}$ of the C_α atoms, the superscript T denotes the transpose, K is a normalization constant, and Γ is the symmetric Kirchhoff or valency-adjacency matrix in graph theory. The elements of Γ are given by

$$\Gamma_{ij} = \left\{ \begin{array}{ll} -\gamma^* & \text{if } i \neq j \text{ and } R_{ij} \leq r_c \\ 0 & \text{if } i \neq j \text{ and } R_{ij} > r_c \\ -\sum_{i \neq j} \Gamma_{ij} & \text{if } i = j \end{array} \right\} \tag{12}$$

The summation for evaluating Γ_{ii} is performed over all off-diagonal elements on the ith column (or row). r_c is the cutoff separation defining the range of non-bonded contacts. The equilibrium correlation between the fluctuations of two sites k and l is obtained from [34, 35]

$$\langle \Delta R_k \cdot \Delta R_l \rangle = (1/Z) \int \Delta R_k \cdot \Delta R_l \, e^{-V/kT} \, d\{\Delta R\} = (3/2)[\Gamma^{-1}]_{kl}$$

where $V = \{\Delta R^T\} \Gamma \{\Delta R\}$ is the potential associated with the vibrations of the C^α-atoms, the angular brackets designate the ensemble average over all fluctuations, and $[\Gamma^{-1}]_{kl}$ is the kl^{th} element of the inverse of Γ. Γ may be regarded as the atomistic counterpart of the stiffness matrix in the analysis of elastic bodies. We also note the similarity between the structures of the matrix Γ and the transition rate matrix **A**, defined in eq (3).

The mean-square fluctuations of HIV-1 protease C^α atoms are displayed in Figure 4 by the solid curve. These are directly found from the diagonal elements of Γ^{-1}. The only adjustable parameter in the theory is γ^*, which is determined by normalizing the theoretical distribution with respect to the experimental, so as to match the areas enclosed by the two curves in each figure.

The agreement between the Gaussian network model and experiments is striking. Similar success was observed for several other proteins[34]. In addition to predicting the Debye-Waller factors accurately, a normal mode analysis of fluctuations permits us to predict the large scale domain motions [24, 37]: The fluctuations induced by the slowest modes indicate the active site and the hinge region, both of which are highly constrained in space and therefore exhibit very small fluctuations, whereas the recognition loop is clearly identified as the largest amplitude fluctuation region of the molecule. The length scale of these cooperatively moving units is in the order of 20 Å. An important issue is whether a careful spatial analysis of mean-square fluctuations, which are readily measurable by Mössbauer scattering, for example, furnishes information on the cooperative dynamics of glasses.

Conclusion

Three different models are proposed to analyze bulk polymer dynamics at different temperature ranges. The dynamic rotational isomeric state model, which applies well above T_g, explains the transition from single exponential to KWW behavior. The cooperative kinematics model describes the cooperative motions around T_g. The Gaussian network model provides new possibilities for analyzing the behavior of bulk polymers well below T_g.

References

1) I. Bahar, B. Erman, *Macromolecules* **20**, 1368 (1987)
2) I. Bahar, B. Erman, L. Monnerie, *Adv. Polym. Sci.* ***116***, 145 (1994)
3) D. B. Adolf, M. D. Ediger, *Macromolecules* **25**, 1074 (1992)
4) R. H. Gee, R. H. Boyd, *J. Chem. Phys.* **101**, 8028 (1994)
5) E. G. Kim, W. L. Mattice, *J. Chem. Phys.* **101**, 6242 (1994)
6) M. D. Ediger, D. B. Adolf, *Adv. in Polym. Sci.* **116**, 73 (1994)
7) I. Bahar, B. Erman, L. Monnerie, *Macromolecules* **25**, 6309 (1992)
8) I. Bahar, B. Erman, L. Monnerie, *Macromolecules* **25**, 6315 (1992)
9) C. Baysal, I. Bahar, B. Erman, L. Monnerie, *Macromolecules* **29**, 2980 (1996)
10) T. Haliloglu, I. Bahar, B. Erman, W.L. Mattice, *Macromolecules* **29**, *8942* (1996)
11) I. Bahar, *Macromol. Theory & Simulations* **6**, 881 (1997)
12) M.-A. Krajewski-Bertrand, F. Laupretre, Personal communication.
13) H. Frauenfelder, A. Petsko, D. Tsernoglou,*Nature* (London) **280**, 558 (1979)
14) J. Colmenero, A. Arbe, G. Coddens, B. Frick, C. Mijangos, H. Reinecke, *Phys. Rev. Lett.* **78**, 1928 (1997)
15) C. Baysal, B. Erman, I. Bahar, F. Laupretre, L. Monnerie, *Macromolecules* **30**, 2058 (1997)
16) I. Bahar, B. Erman, L. Monnerie, *Macromolecules* **23**, 3805 (1990)
17) I. Bahar, B. Erman, F. Kremer, E. W. Fischer, *Macromolecules* **25**, 816 (1992)
18) I. Bahar, B. Erman, G. Fytas, W. Steffen, *Macromolecules* **27**, 5200 (1994)
19) I. Bahar, N. Baysal, B. Erman, L. Monnerie,*Macromolecules* **28**, 1038 (1995)
20) C. Baysal, I. Bahar, B. Erman, L. Monnerie,*Macromolecules* **29**, 2510 (1996)
21) N. E. Moe, M. D. Ediger, *Polymer* **37**, 1787 (1996)

22) D. Schaefer, H. W. Spiess, U. W. Suter, W. W. Fleming, *Macromolecules* **23**, 3431 (1990)

23) E. E. Abola, F. C. Bernstein, S. H. Bryant, T. F. Koetzle, J. Weng, J.: in "Crystallographic Databases-Information Content Software Systems, Scientific Applications", edited by F. H. Allen, G. Bergerhoff and R. Sievers, Data Commision of the International Union of Crystallography, Bonn, Cambridge and Chester, 1987, **107.**

24) I. Bahar, A. R. Atilgan, M. C. Demirel, B. Erman, *Phys. Rev. Lett.* **80**, 000 (1998)

25) C. A. Angell, *Science* **267**, 1924 (1993)

26) J. L. Green, J. Fan, C. A. Angell, *J. Phys. Chem.* **98**, 13780 (1994)

27) H. Frauenfelder, G. S. Sligar, P. G. Wolynes, *Science* **254**, 1598 (1991)

28) A. W. Kauzmann, *Chem. Rev.* **43**, 219 (1948)

29) J. Colmenero, A. Arbe, R. Alegria, *Phys. Rev. Lett.* **71**, 2603 (1993)

30) D. Theodorou, U. W. Suter, *Macromolecules* **18**, 1985 (1985)

31) M. M. Tirion, *Phys. Rev. Lett.* **77**, 1905 (1996)

32) M. Levitt, C. Sander, P. S. Stern, *J. Mol. Biol.* **181**, 423 (1985)

33) P. J. Flory, *Proc. R. Soc. Lond. A.* **351**, 351 (1976)

34) I. Bahar, A. R. Atilgan, B. Erman, *Folding & Design* **2**, **173**, (1997)

35) A. Kloczkowski, J. E. Mark, B. Erman, *Macromolecules* **1423**, 1423 (1989)

36) D. S. Pearson, *Macromolecules* **10**, 696 (1977)

37) T. Haliloglu, I. Bahar, B. Erman, *Phys. Rev. Lett.* **79**, 3090 (1997)